Journal of Power Sources 196 (2011) 587–595

Contents lists available at ScienceDirect

Journal of Power Sources

journal homepage: www.elsevier.com/locate/jpowsour

Ultracapacitors for fuel saving in small size hybrid vehicles☆

L. Solero[a,*], A. Lidozzi[a], V. Serrao[a], L. Martellucci[b], E. Rossi[c]

[a] University ROMA TRE, Dept. of Mechanical and Industrial Eng., Via della Vasca Navale, 79 – 00146 Roma, Italy
[b] University of Rome "La Sapienza", Dept. of Electrical Eng., Via Eudossiana, 18 – 00184 Roma, Italy
[c] ENEA, Via Anguillarese, 301 – 00060 S. Maria Galeria, Roma, Italy

ARTICLE INFO

Article history:
Received 30 April 2009
Received in revised form 9 July 2009
Accepted 21 July 2009
Available online 3 August 2009

Keywords:
Power electronic converter
Control strategy
Permanent magnet electrical machine
Genset

ABSTRACT

The main purpose of the paper is to describe a small size hybrid vehicle having ultracapacitors as on-board storage unit. The vehicle on-board main power supply is achieved by a genset being formed of a 250 cm^3 internal combustion engine and a permanent magnet synchronous electric generator, whereas 4 16V-500F ultracapacitors modules are connected in series in order to supply as well as to store the power peaks during respectively acceleration and braking vehicle modes of operation. The traction power is provided by a permanent magnet synchronous electric motor, whereas a distributed power electronic interface is in charge of all the required electronic conversions as well of controlling the operating conditions for each power unit. The paper discusses the implemented control strategy and shows experimental results on the modes of operation of both generation unit and storage unit.

1. Introduction

Present researches concerning electric vehicles (EV) and hybrid-electric vehicles (HEV) concentrate in the search for a compact, lightweight, and efficient energy storage system that is both affordable and has acceptable cycle life. The traction system is usually composed by electric motor, inverter, and associated control circuitry and it is not the limiting factor to obtain high performance and to permit large-scale production of such vehicles [1–4]. Electric power storage and generation units are whilst worthy of extended investigation in order to reduce size and weight, as well to increase reliability and vehicle long distance capability [5,6].

Attention is now increasingly focused on fuel cell (FC) and hybrid technologies as a way of producing breakthrough vehicles with alternative power plants. A number of automakers see fuel cell powered vehicles (FC-EV) as the ultimate route to achieving sustainable long-term alternative propulsion systems [7]. A number of drive-train architectures have recently been proposed to combine two or more on-board generation units (GU) and storage units and to overcome constraints related to fuel consumption, pollution, vehicles long distance capability. Interfacing of traction drive requirements with on-board GU and storage unit characteristics and modes of operation calls for suitable power electronic converter configuration and control [8–12].

In terms of power sources, the proton exchange membrane FCs are being increasingly accepted as the most appropriate supply for EVs because they offer clean and efficient energy without penalizing either performance or driving range. However, today technology and cost limits make FC generators not yet appropriate for commercial small size vehicles, which require reliable and affordable technologies. As a consequence, use of internal combustion engine (ICE) based gensets is still a convincing solution for providing needed on-board power supply to drive electric and hybrid vehicles. Unfortunately, this solution is responsible of almost same fuel consumption and pollution of traditional vehicles when auxiliary storage systems are not included; the auxiliary storage unit is in fact responsible for running the ICE at favorable conditions acting as power/energy buffer and making the ICE operating conditions almost independent from traction requirements.

As a consequence, ultracapacitors as auxiliary on-board storage unit are investigated in the paper with reference to a ICE small size hybrid vehicle. In the proposed vehicle, a 250 cm^3 ICE and a permanent magnet (PM) synchronous electric generator are directly coupled in order to form a genset as the on-board main power supply, 4 ultracapacitors modules being rated 16V-500F are connected in series in order to supply and to store the power peaks during respectively acceleration and braking. The required traction power is provided by a permanent magnet synchronous electric motor (PMSM), whereas a distributed power electronic interface has been designed to accomplish all the required electronic conversions (i.e. ac–dc for the generation unit, dc–dc for the storage unit, dc–ac for the traction unit) as well to control the operating conditions of each power unit.

☆ Presented at 3rd European Symposium on Supercapacitors and Applications, Rome, Italy, 6–7 November 2008.

* Corresponding author. Tel.: +39 06 57333277; fax: +39 06 5593732.
E-mail address: solero@uniroma3.it (L. Solero).

0378-7753/$ – see front matter © 2009 Elsevier B.V. All rights reserved.
doi:10.1016/j.jpowsour.2009.07.041

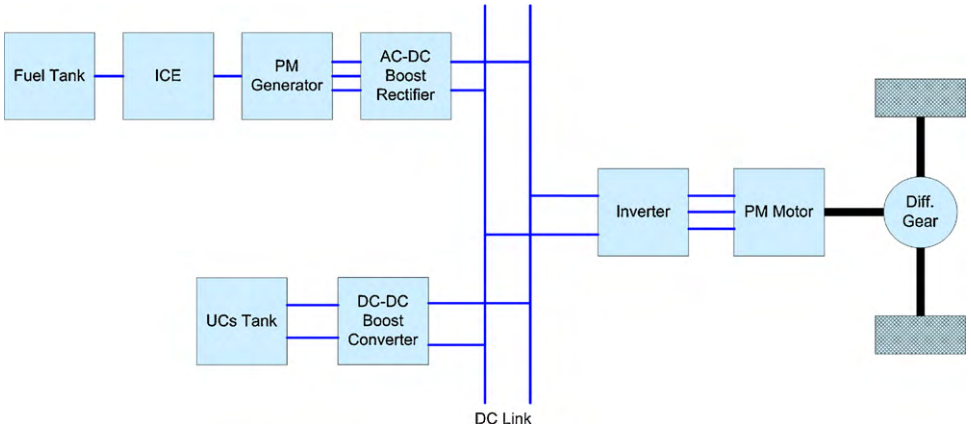

Fig. 1. Vehicle proposed power train configuration.

The paper is organized as follows: description of the vehicle power train as well of each power unit is given in Section 2, Section 3 summarizes the achieved ICE optimization, description of the control strategy for both the generation unit and the storage system is given in Section 4. Achieved simulation and experimental results, on the basis of the different modes of operation which can occur as a consequence of the proposed running driving cycle, are shown in Section 5, together with the carried out experimental activity, concerning the testing of the components to be mounted on-board the vehicle; finally, conclusions are given in Section 6.

Table 1
Vehicle performances specifications.

Operating weight, driver not included [kg]	500
Maximum speed [km h^{-1}]	70
Maximum acceleration [m s^{-2}]	1.35
Maximum climbing for 30 m length run	17%
Cooling system	Liquid
hybrid configuration	Series
Internal combustion engine size	250 cm^3
Fuel consumption	2.5 l per 100 km
Emission class	Euro III, Euro IV in case of liquid propane fuel

2. Vehicle power train

Parking difficulties and increasing density of road traffic are indirectly promoting proliferation of small size vehicles in large cities as Rome, Italy. Unfortunately, these vehicles are usually not optimized for either pollution reduction or for fuel saving, besides both pollution reduction and fuel saving are even more essential characteristics of today and future vehicle technology. A hybrid power train with ultracapacitors included is proposed in the paper with the purpose of fuel saving and pollution reduction in small size vehicles.

Ultracapacitors are electrical energy storage devices, which offer high power density, extremely high cycling capability and mechanical robustness. Recent technology improvements enabled ultracapacitors (UCs) to be an interesting option for short-term high power applications, such as in industry, automotive and traction drives, regenerative energy systems, medical and telecommunication equipment. The latest UCs can outperform batteries in several key performance parameters such as power density (5 kW kg^{-1}), cycle life (>100,000 cycles), temperature sensitivity, and dynamic behavior [13,14]. As the UC technology improves further, an impressive world of applications should emerge. These applications include storage of intermittent energy from solar and wind sources, bulk power system peak shaving, APU for automotive systems, load leveling in hybrid and electric vehicles, power buffering in elevators [15].

UCs appear to be very promising in particular for applications concerning hybrid and electric vehicles (HEVs), in fact, an UC module is capable of very fast transients in its output current, thus making this storage unit very suitable for electric traction applications where high current values and high dynamic behavior are required during acceleration and regenerative braking. However, in spite of reaching thousands of Farads, the UCs support very low voltages (1–2.7 V); as a consequence a stack of series-connected UCs can produce an equivalent UC module of tens of Farads that is able to hold up tens of Volts, in addition UC modules offer voltage value at terminals which is almost directly proportional to their state of charge (SOC) and therefore greatly dependent on UC operating condition. A power electronic converter is then required for conveniently utilise UC modules in the mentioned applications [16,17], besides reliable converter topologies as well high dynamic control techniques should be chosen in order to best operate the UC storage unit. To this purpose, output voltage control is commonly required for the UC power electronic converters in order to balance sudden and deep variations either in the load or in the system main power source.

The proposed vehicle power train is shown in Fig. 1 and design specification for the small size vehicle is stated in Table 1. Each power electronics converter makes use of the module Semikron SKAI 5001 MD15, which is based on MOSFET technology, and main characteristics of assembled genset, traction motor, UCs tank, and distributed power electronic interface are respectively listed in Tables 2–6.

Pictures of the vehicle during its recent presentation at the Bologna Motor Show 2008 are shown in Figs. 2 and 3, which respectively show UC tank and traction motor in the vehicle front view and the genset system in the vehicle rear view.

Table 2
ICE Characteristics.

Manufacturer	PIAGGIO
Type	Spark Ignition, QUASAR family
Displacement [cm^3]	244.3
Bore size [mm]	72
Stroke [mm]	60
Cooling	Liquid cooled
Timing	4 valves—SOHC
Max Power (@ 8250 rev min^{-1}) [kW]	16.2
Max Torque (@ 6500 rev min^{-1}) [Nm]	20.2
Injection	Electronic
Weight [kg]	36
Emissions level	EURO 3
Catalytic converter	3 Way

Table 3
PM generator characteristics.

RMS line-to-line EMF (@ 5000 rev min^{-1}) [V]	55
Rated torque [Nm]	20
Maximum rotational speed [rev min^{-1}]	5000
Poles pairs	3
Line-to-line resistance [Ω]	0.087
Line-to-line inductance [mH]	0.096
Permanent magnets	NdFeB
Iron losses [W kg^{-1}]	1.7
Total weight [kg]	25
Cooling system	Water

Table 4
PM traction motor characteristics.

RMS line-to-line EMF (@ 4600 rev min^{-1}) [V]	55
Rated torque [Nm]	30
Maximum rotational speed [rev min^{-1}]	4600
Poles pairs	4
Line-to-line resistance [Ω]	0.040
Line-to-line inductance [mH]	0.058
Permanent magnets	NdFeB
Iron losses [W kg^{-1}]	1.7
Total weight [kg]	23
Cooling system	Water

Table 5
UCs tank characteristics.

Capacitance [F]	125
Rated voltage [V]	64.8
ESR DC [mΩ]	10
ESR 1 kHz [mΩ]	8.4
Maximum power [kW kg^{-1}]	5.4
Rated power [kW kg^{-1}]	2.1
Weight [kg]	23
Operating temperature range [°C]	40–65

Table 6
Distributed power electronic converter characteristics.

Building block module	Semikron SKAI 5001 MD15 1420W
Device maximum voltage [V]	150
Device maximum current [A]	400
MOSFET on resistance @ Tj = 125 °C [mΩ]	3.39
Switching energy (Eon + Eoff) at I = 300 A [mJ]	5.1
Total dc-link capacitance [mF]	3 × 9
UC-side inductors [μH]	2 × 39
Overall size [mm × mm × mm]	3 × 315 × 115 × 95
Total weight [kg]	3 × 3
Cooling system	Water

Fig. 2. Bologna Motor Show 2008: vehicle prototype front view.

Fig. 3. Bologna Motor Show 2008: vehicle prototype left side-rear view.

3. Ice optimization

In order to achieve a light, modern and efficient generator set, an ICE with characteristics of Table 2 and derived from the scooter market has been considered.

The maximum power output is higher than the power needed for the investigated application; however, the maximum power is achieved at high revolution speed (8500 rev min^{-1}) that was not considered for the generator set because of noise emission reasons, in order to avoid high revolution speed the choice of a less powerful engine has been rejected. In fact, the characteristics of lightness, emissions level and overall engine design quality assured by the selected 250 cm^3 engine are not typical of smaller engines, in many cases less sophisticated and efficient.

The selected engine has been optimized for the generator set mode of operation by modifying some characteristics as inlet and outlet manifold length, valve timing, compression ratio, injection timing. Further, in order to implement ICE load remote control, a motorized throttle body has been designed and installed on the inlet duct, without compromising the original manifold design and leaving untouched the throttle position sensor utilised by the engine injection control unit. In order to perform the efficiency optimization of the ICE, a redesign strategy of the engine was defined; a fine tuning was considered to this purpose, avoiding major modifications to the engine base structure.

A first simple analysis was performed by considering engine modifications only to the intake manifold length, exhaust manifold length and compression ratio. These modifications were performed with simple and cost effective operations. The most significant parameter, as expected, is the compression ratio, which can cut up to 5% of fuel consumption when approaching the higher values being considered (minimum fuel consumption rate equal to 239 g kW h^{-1}).

A further step forward in the optimization analysis of the engine was achieved by considering more invasive modifications to ICE valves diameters and exhausts conducts size; the achieved fuel consumption best operating point results 232.8 g kW h^{-1} at 4000 rpm as revolution speed, with full open throttle (85°). These results show a further 5% cut of the fuel consumption in comparison with the achieved first optimization result.

4. Generation unit and Storage System Control Strategy

The control system of the entire on-board propulsion system is designed as four different subsystems which communicate through the Controller Area Network (CAN) following the CAN 2.0A spec-

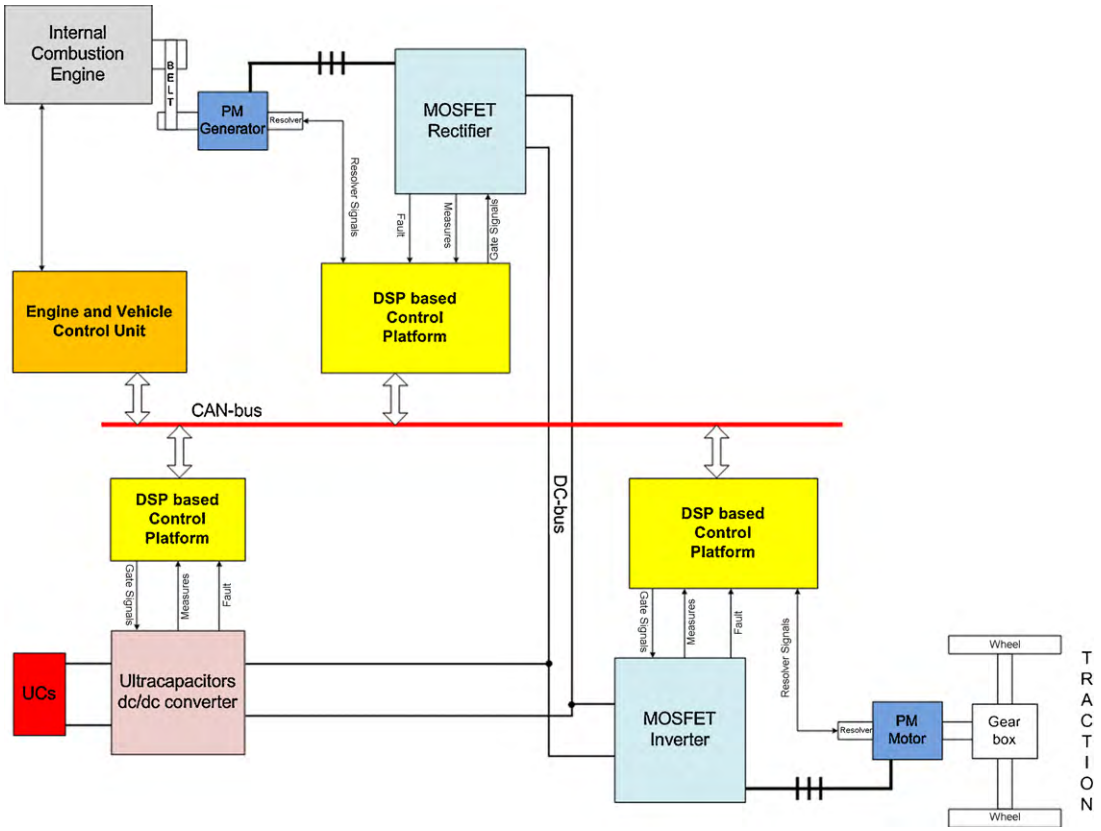

Fig. 4. MicroCar Schematic Control System.

ifications at data rate of 1 Mbit s^{-1} [18]. The four subsystems are shown in Fig. 4 and identified as Generation Unit control, Ultracapacitors control, Traction Motor (TM) control, and Engine and Vehicle control unit [19].

The power electronic converters are controlled in order to supply the dc-link according to the traction power demand; however, each on-board source should feed the power on the basis of their own characteristics. Thus, the Vehicle control unit is responsible for the control references generation in order to appropriately share the power flow on the basis of UC state of charge, the efficiency map and the per second maximum current variation of the generation unit. Dynamic behavior of the transient variations of the power supplied by the generation unit is limited in order to improve ICE efficiency as well to reduce polluting emissions. However, the power exchange among generation unit, storage unit and traction unit is accomplished at constant dc-link voltage, as a result the power supplied by the generation unit can be controlled by means of current regulation. In fact, current control is adopted for the GU converter; as a result, appropriate controlled dynamic response during acceleration and braking of the vehicle is achieved for the operating point variation of the ICE. Furthermore, desired dc-link voltage level is accomplished in every working condition by operating on UC-side converter; as a consequence UC unit is responsible for the traction drive dynamic behavior fulfillment. In conclusion, UC converter is voltage controlled and its control structure is designed to keep the dc-link voltage at 84 V. In the following a more detailed description of the control system is given.

The GU control must be able to start the ICE up to its idle speed. After that, when the requested power is different from zero, the electric generator will supply power toward the 84 V common dc-bus. It means the electric machine works as a motor to start the ICE and as a generator during the normal mode of operation. The transition between these two modes is accomplished avoiding discontinuities. In fact, machine control is based on the Field Oriented Control (FOC) algorithm [20] and a resolver is used to acquire the rotor speed and position. Modulation scheme is the 3-phase centered Space Vector Modulation, which has been chosen in order to reach low Total Harmonic Distortion (THD) and torque ripple [21]. The control program is implemented on a 16 bits fixed-point Digital Signal Processor (DSP) from Analog Devices. The communication between the position transducer interface and the DSP is accomplished by the SPI (Serial Peripheral Interface) serial standard from Motorola.

An extensive simulation activity has been carried out in order to investigate average and peak power requirements for the proposed propulsion system. Typical driving performances of conventional microcars have been considered as well several standardized urban driving cycles such as ECE UDC, FTP 72 and JC08 cycles have been analyzed. Based on the energy requirements simulation results, the MicroCar typical requested transient power can be supplied by a storage system, which is able to deliver almost 10 kW for 20 s. It means a capacitance around 125 F for the Ultracapacitors tank with reference to the rated voltage of 64 V. During the different modes of operation, such as acceleration, regenerative braking and cruising speed, UC voltage varies between 32 V and 64 V depending on SOC and the UCs tank parasitic resistance which is about 10 mΩ. As a consequence, at minimum voltage level the maximum current requested to the UCs is expected to be 320 A. The quite large amount of peak current requires the selection of parallel connection of two bidirectional dc–dc Boost converters in order to connect the Ultracapacitors to the dc-link; the chosen topology is able to supply power with output voltage higher than input voltage during motoring mode of operation, as well it is able to supply power in the reverse way during braking mode of operation with output voltage lower than input voltage [22]. The traction drive requested transient current is evenly shared between the two dc–dc Boost

power converters; anyway, all of them co-operate to keep the dc-link voltage at 84 V.

Bidirectional dc–dc Boost converters are used in step-up mode of operation in order to transfer energy from UC tank to the dc-link, whereas step-down operation is used to charge UC tank and to recover the braking energy. The selected bidirectional topology is suitable to connect power sources, in which the voltage level is load and/or state of charge dependent, at lower voltage level with respect to traction electric drives, which are usually fed at high voltage in order to reach high efficiency; on the contrary, in UC tanks and battery systems the number of elements connected in series is usually limited to improve the system reliability.

Each dc–dc boost converter is composed of two controlled switches (MOSFET), two power diodes, one input inductor and one output capacitor. The power semiconductors of each converter are connected to form a phase-leg; thus, these four components can be purchased as a single three-terminal assembly. Furthermore, in the proposed solution all the semiconductor devices can be obtained as one six-pack MOSFET module, where three phase-legs are included, then reducing the converter overall dimensions. As a consequence, two phase-legs are directly used to achieve the two bidirectional dc–dc boost converters, whereas the remaining phase-leg is used to dissipate onto a braking resistor the dc-link power in excess during regenerating, in case the UC tank is already fully charged.

In UC power stage converter, switches operate in complementary way thus the bidirectional converter works always in continuous conduction mode (CCM) and it promptly compensates the dc-link voltage unbalances. Whole system stability, dynamic behavior and both current and voltage loops performances have been investigated through simulation models, Fig. 5 shows the circuital model of UC power stage and its control loops for each dc–dc Boost converter.

The dc–dc Boost converter is a non-linear time variant system. Many control solutions have been proposed in literature. Double loop linear control has been selected as control strategy. The inner loop is responsible for the current regulation and the outer voltage loop keeps the dc-link voltage constant. Linear control design procedure requires the system to be linearized around a particular selected operating point. This means that when the system works on the linearization point it is stable and has the investigated behavior. In any different operating condition, stability and behavior must be verified. For this reason, the operating point for UC unit control tuning has been chosen to be the worst working condition. Load current is chosen equal to the maximum value (160 A for each dc–dc converter) and duty cycle are set to the highest value (65%) (i.e. when the UCs SOC reaches the minimum value). Two paralleled phase-legs compose the UCs system; hence, the current in each phase-leg must be controlled separately by means of two independent current regulators.

The simplest and reliable way to control the inner current loops is to use Proportional-Integral (PI) regulators. The integral term assures the system to reach the reference value whereas the proportional gain increases its performance. The operating point (i.e. the linearization point) has been selected according to the step-up mode of operation converter transfer functions. The most critical aspect is the presence of a Right Half Plane-Zero (RHP-Z) which is strictly dependent to the load current; when the load current increases, as well the converter duty cycle increases, the RHP-Z moves closer to the control frequency. This behavior causes a reduction of the stability margin or in the worst case the system instability. It is found that converter inductance, as well remain-

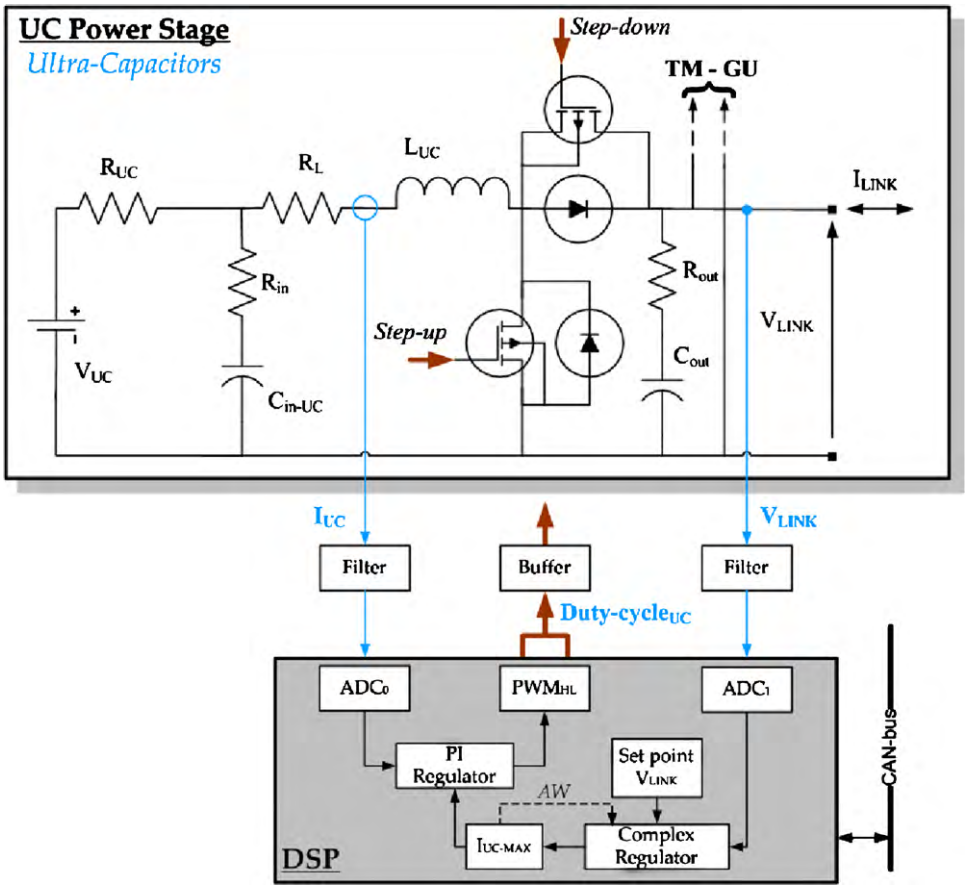

Fig. 5. UC power stage and control loops.

ing converter parameters, such as output capacitance, switches and diodes characteristics, do not affect significantly the RHP-Z location.

As previously mentioned, the Ultracapacitors control architecture has an outer voltage loop which task is to maintain the dc-link voltage at 84 V, a double control loop structure is then required [23]. Voltage compensator design needs the current loop to be closed. The design procedure is the same as discussed for the current loop. In this case, the controller structure is more complicated because it must be optimized for load variations, as a consequence the derivative action should be added to the regulator. Voltage loop compensator is a second order system; the first pole is in the origin (pure integral action) whereas the second pole has been added to make it physically feasible. The high frequency pole has been added according to the frequency value of $1/(T_d/N)$ where T_d is the derivative term time constant and N is a coefficient devoted to filter the derivative action. N has been set to 20 as a trade off between load unbalances compensation speed and noise filtering.

The vehicle management system is in charge for assessing the instantaneous reference values of power flows for TM, GU and UC. The vehicle driver, through the acceleration pedal, decides the traction motor operating point in terms of torque and then also of rotational speed; a variation of the position of the acceleration pedal produces a torque variation of the electric motor which is supplied by the power inverter, as a consequence change of the electric power value is experimented at the dc-link. Power variations mean electric current variations at constant voltage dc-link; for this reason, the generation unit is controlled by a reference which follows the dc-link current changes. However, the dc-link current variations are dependent on vehicle dynamics in terms of accelerations and braking, transients which are not congruent with the desired fuel low consumption as well reduced emissions modes of operation which are expected for the proposed genset. For this reason, the dc-link current transients are filtered by means a low pass Butterworth filter, the filter output is the reference for the AC–DC Boost Rectifier which is responsible for the genset modes of operation; the filter crossover frequency is set in order to reach the envisaged fuel consumption and emissions. As a result, the current supplied by the generation unit follows the dc-link current transients at low dynamic and the dc-link voltage either reduces or increases, with respect to 84 V, during respectively accelerations and braking. The dc-link voltage variation is used as control reference for the ultracapacitors unit, which is regulated in order to supply the required power and to recover the available regenerative braking during transients. The vehicle management system adjusts the low pass filter bandwidth as a function of the UCs state of charge, in fact the storage unit is well capable of either supplying power during accelerations or recovering energy during braking provided respectively high and low SOC, as a consequence low bandwidth for the genset reference current is demanded; whereas, the bandwidth is increased for intermediate SOC conditions. The vehicle management system is also in charge for controlling the storage system SOC on the basis of two reference values, the maximum SOC and the minimum SOC; the mentioned SOC limits are adjusted as a consequence of the vehicle speed with the purpose of complying with the dc-link power during the vehicle transients.

5. Experimental results

The achieved main components characterization allowed modelling of the whole vehicle as well the identification of an appropriate control law in order to suitably manage both the generation unit and the storage unit. The investigation of the proposed hybrid system was firstly carried out by means of simulations referred to conventional urban driving cycles with the purpose of defining both the value for the low pass filter bandwidth used for generating the genset reference current and the values for the real-time calculation of upper and lower SOC references as a function of the vehicle speed. Then, the prototypal system has been tested along with an experimental driving cycle, which was achieved through instrumentation directly installed on a small size vehicle being driven along the center of the city of Rome. The driving cycle lasts about 1000 s with a speed peak value of 66 km h^{-1} as shown in Fig. 6. The experimental results have been achieved by measuring current and voltage levels for the different storage and generation units, as well for the distributed power electronic converter.

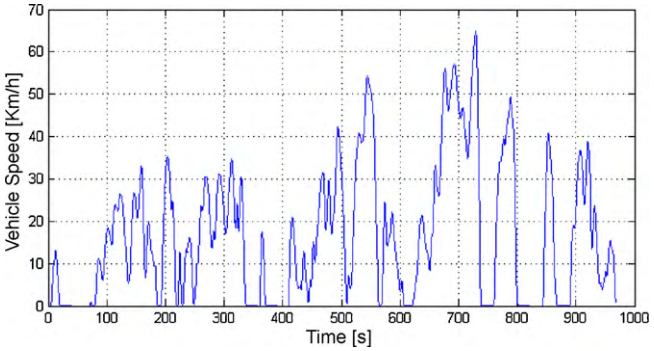

Fig. 6. Experimental driving cycle.

The traction electric drive requires the power supply being depicted in Fig. 7, which is related to the dc-link value of 84 V. The power peak value is slightly higher than 12 kW, whereas the regenerative electric power shows a peak value of 8 kW, being the braking function accomplished both electrically and mechanically according to a suitable repartition between the two braking systems.

Power value at the dc-link is used by the control system in order to provide the reference for the operating point of the generation unit, any variation of the required power is conditioned through the low pass filter in order to avoid fast transients for the ICE which would occur in bad efficiency and high exhausts emissions, the difference between the required traction power and the generated power is covered by the ultracapacitors unit. Fig. 8 shows a detailed portion of the on-board power management, whereas Fig. 9 depicts a zoom view of the supplied and required current at dc-link; each dc-link required current variation is accomplished by the UC tank during first transients, whereas the GU operating points are changed at lower dynamic according to the ICE efficiency map. The chosen bandwidth for the low pass filter is 0.5 rad s^{-1}, which means that, under a step variation, the genset current reference reaches its steady state value in about 8 s; the value of the bandwidth has been chosen following the trial and error procedure with

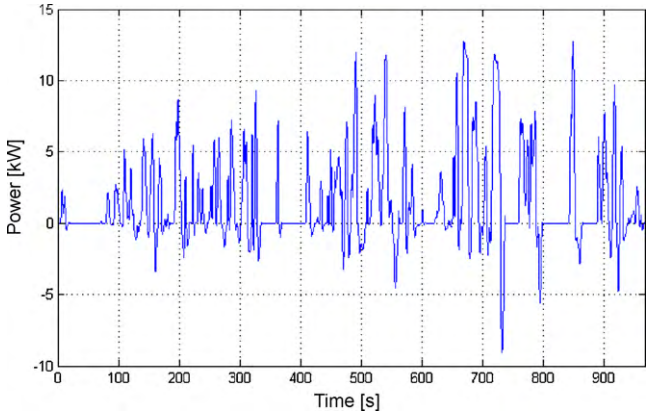

Fig. 7. Electric power at dc-link.

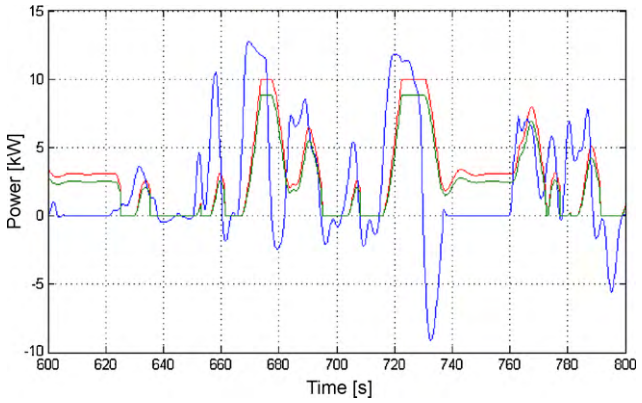

Fig. 8. Detail of the traction electric power at dc-link (blue), ice mechanical power (red), generated electric power at dc-link (green). (For interpretation of the references to color in this figure caption, the reader is referred to the web version of the article.)

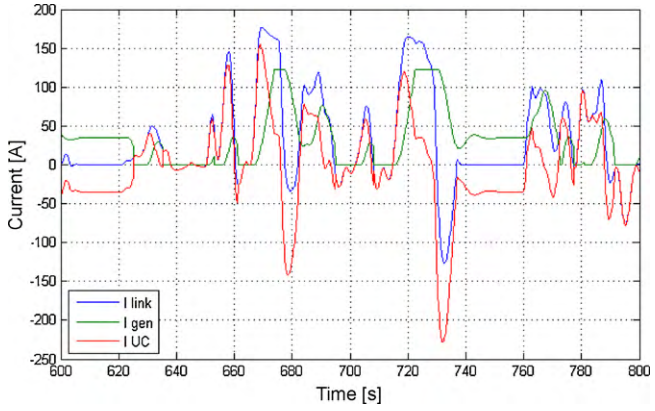

Fig. 9. Detail of the dc-link required current (blue), GU supplied current at dc-link (green), UC supplied current at dc-link (red). (For interpretation of the references to color in this figure caption, the reader is referred to the web version of the article.)

the purpose of assuring the required transient modes of operation of the vehicle and, at the same time, the slowest as possible dynamic for the on-board generation system together with proper UCs state of charge operating range (0.5–0.95).

Fig. 10 shows the UCs unit state of charge along the driving cycle. UCs SOC is managed in order to assure enough power during vehicle accelerations as well the desired recovered power during braking. To this purpose, SOC is controlled on the basis of two reference

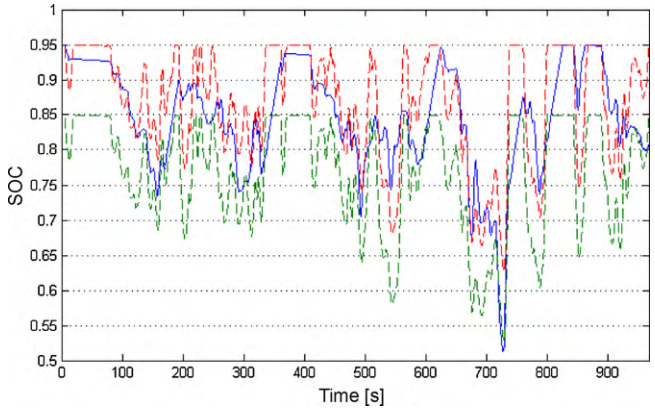

Fig. 10. UCs Unit State of Charge (blue), maximum SOC reference (red), minimum SOC reference (green). (For interpretation of the references to color in this figure caption, the reader is referred to the web version of the article.)

Fig. 11. Power electronics modular element.

values, the maximum SOC and the minimum SOC; whenever the state of charge is either higher or lower than the mentioned limits the UCs unit is consequently discharged or charged. The selected strategy considers the variation of SOC limits as a consequence of the vehicle speed, in fact at high speed the UCs unit must be able to recover the power available through a braking action, whereas at low speed the storage unit must be able to provide the required power for accelerations.

Achieved results show that lower dynamic behavior for the GU as well management of UCs SOC at fixed upper and lower reference values (i.e. not dependant with the vehicle speed) would produce an irreversible storage unit discharge as well the risk to fail the traction requirement during intense accelerations; instead, the chosen speed dependent SOC strategy properly controls the storage system. In fact, UC SOC level does not show significant difference between the end and the beginning of the investigate driving cycles, as well at the most critical point (720–730 s) of the experimental driving cycle it can be recognized the UCs are still over the bottom level of their SOC range. The used parameters in the control system allow to reach a fuel consumption of almost 2.6 l per 100 km, which is a significant improvement with respect to 3–3.5 l per 100 km of the conventional ICE small size vehicles. A further improvement in fuel consumption is achieved when even lower transients could be accepted for the genset (i.e. filter lower bandwidth), to this purpose larger sized UCs storage system should be used, however increasing of the storage unit volume and weight should be also considered.

An extensive activity has been also carried out with the purpose of experimentally characterize the main electrical and electronic components which form the proposed vehicle powertrain.

The modular element used to accomplish the distributed power electronic interface is shown in Fig. 11, whereas the assembled control board is visible in Fig. 12. The control board has been designed in order to be positioned directly on the top side of the power electronics modular element.

Phase current waveform is shown in Fig. 13 for the electric generator, the electric generator resolver waveform is also plotted to assure the correct timing of the phase current with the position of the electrical machine rotor. Phase current waveform shows a quite sinusoidal behavior with very low Total Harmonic Distortion

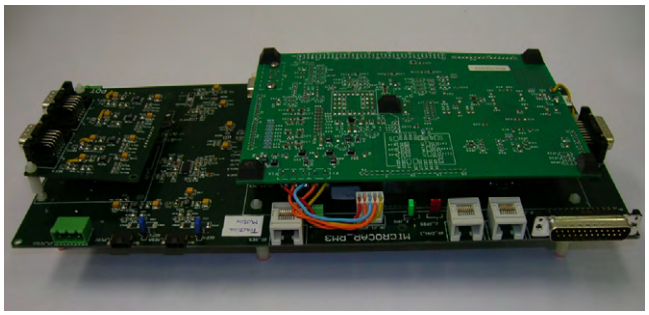

Fig. 12. Control board.

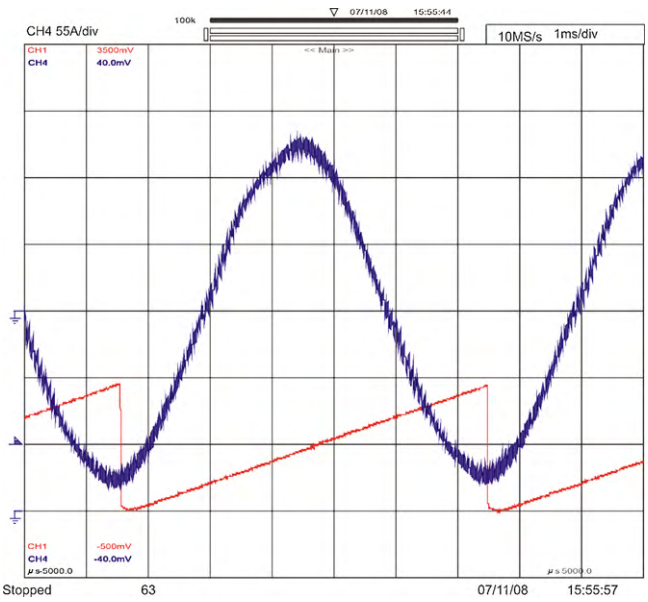

Fig. 13. Electric motor phase current (55 A div^{-1}, 1 ms div^{-1}) at 3350 rpm and 17 Nm operating condition.

(THD), as a consequence very low torque ripple is experimented at the electric generator shaft.

Similar experimental results were achieved for the electric motor which is responsible for the traction function. UCs unit power electronic converter input current is depicted in Fig. 14 when the dc-link voltage and current are respectively 84 V and 55 A, the UCs voltage was 40 V (i.e. SOC was 0.625). Experimental testing has been carried out for several different operating conditions in terms of speed and torque as far as it concerns both the traction electric drive and the generation unit, as well for several different operating conditions in terms of different UCs SOC and load current as far as it concerns the storage unit power electronic converter.

Results achieved by means of the testing activity allowed to characterize the efficiency of the components being installed on board the vehicle. Efficiencies of respectively the Boost Rectifier, being used to interface the electric generator with the dc-link, the electric generator and of the whole generation unit electric drive

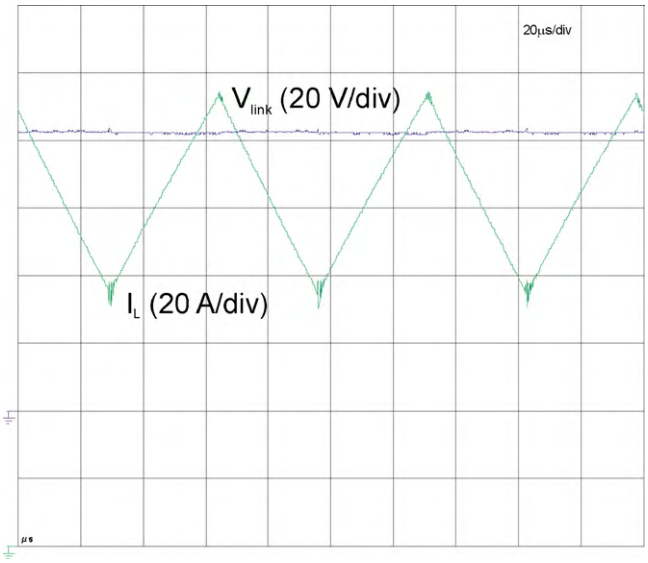

Fig. 14. UCs unit power electronic converter input current (20 A div^{-1}, 20 µs div^{-1}) at 0.625 UCs SOC and 84 V dc-link.

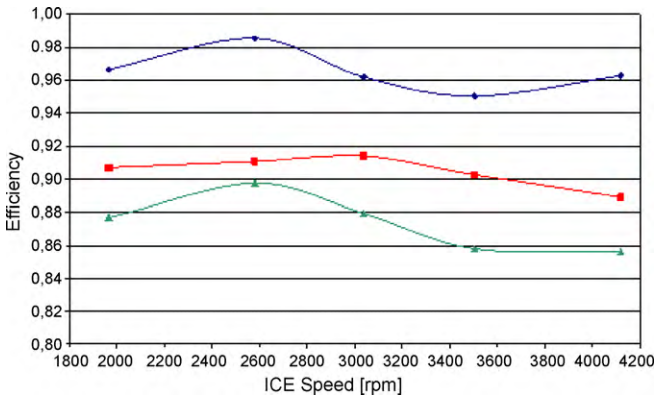

Fig. 15. Generation unit electric drive efficiency vs. ICE speed at 20 Nm (Boost Rectifier—blue trace, electric generator—red trace, electric drive—green trace). (For interpretation of the references to color in this figure caption, the reader is referred to the web version of the article.)

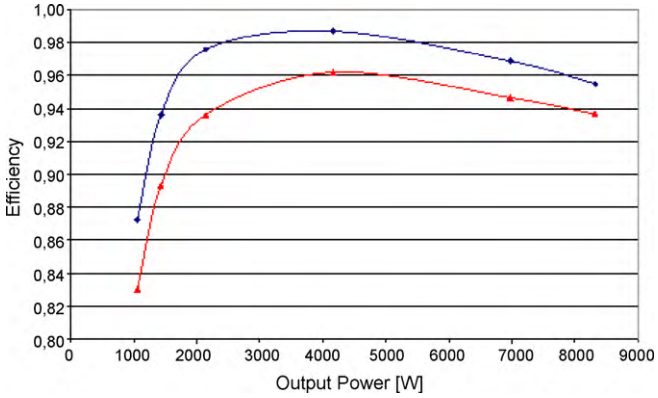

Fig. 16. UCs unit power electronic converter efficiency vs. output power (UCs SOC 0.94—blue trace, UCs SOC 0.625—red trace). (For interpretation of the references to color in this figure caption, the reader is referred to the web version of the article.)

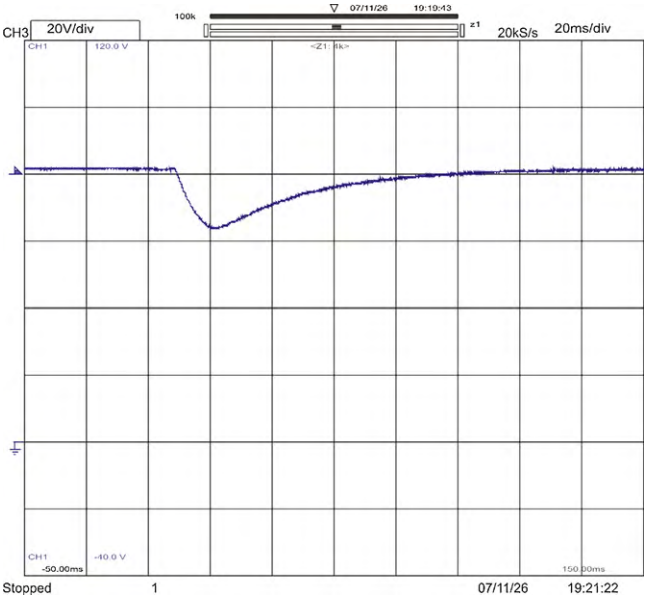

Fig. 17. dc-link voltage transient at 0–50 A load step current and 0.625 UCs SOC (20 V div^{-1}, 20 ms div^{-1}).

are illustrated in Fig. 15 as a function of the ICE speed with a constant torque of 20 Nm. Similar results have been achieved for the traction drive. Experimental efficiency of the UCs power electronic converter is shown in Fig. 16 respectively at 0.94 and 0.625 UCs SOC as a function of the required output power.

Both the electric drives show efficiency close to 90%, where improvement of about 2% can be achieved by enhancing the active materials (mainly the permanent magnets characteristics) of the electric machines; whereas the power electronic converter for the storage system performs at least 95% of efficiency for a quite large range of the operating power values.

Experimental activity was also carried out in order to test the transient behavior of the dc-link voltage during load step variation; in fact, the UCs unit is responsible for the dc-link voltage which is set at 84 V, and the control loops of the UCs unit power electronic converter was designed in order to assure high dynamic performances to the storage system. Fig. 17 depicts the voltage transient when a load step current 0–50 A is directly applied to the dc-link, the test was performed at 0.625 UCs SOC and it is proved that the dc-link voltage level is completely recovered in less than 80 ms. The good performances achieved for each single component are fundamental in order to reach the consumption target of 2.5 l per 100 km.

6. Conclusions

The paper presented a small size hybrid vehicle having ultracapacitors as on-board storage unit. Simulations and experimental activity were carried out with the purpose of characterizing the power components being installed onto the vehicle; internal combustion engine, electric generator, ultracapacitors, electric motor, as well the distributed power electronic interface were investigated in order to reach good performance, which in terms of fuel consumption is expected to be 2.5 l per 100 km. The transient behavior of the power system was also analyzed in order to show the dynamic characteristics of both storage unit and power electronic interface. The MicroCar prototype has been presented at the Bologna Motor Show and future developments will be focused on testing the vehicle at rolling test bench with several driving cycles in order to experimentally verify the fuel consumption at various operating conditions.

References

[1] Z.Q. Zhu, D. Howe, Proceedings of the IEEE, vol. 95, Issue 4, April, 2007.
[2] Z.J. Shen, I. Omura, Proceedings of the IEEE, vol. 95, Issue 4, April, 2007.
[3] A. Emadi, K. Young Joo Lee, Rajashekara, IEEE Transactions on Industrial Electronics 55 (6) (2008).
[4] Y. Xiong, X. Cheng, Z.J. Shen, C. Mi, H. Wu, V.K. Garg, IEEE Transactions on Industrial Electronics 55 (June (6)) (2008).
[5] T.H. Ortmeyer, P. Pillay, Proceedings of the IEEE, vol. 89, Issue 12, December, 2001.
[6] W.D. Jones, Spectrum IEEE 42 (July (7)) (2005).
[7] J. Voelcker, Spectrum IEEE 41 (March (3)) (2004).
[8] F. Crescimbini, L. Solero, Proceedings of COBEP 2005, Recife, Brasil, June, 2005, cd-rom.
[9] S. Lu, CorzineF K.A., M. Ferdowsi, IEEE Transactions on Vehicular Technology 56 (4) (2007), Part 1.
[10] Y. Gao, M. Ehsani, IEEE Transactions on Power Electronics 21 (3) (2006).
[11] G.-J. Su, L. Tang, IEEE Transactions on Power Electronics 22 (6) (2008).
[12] A. Vahidi, A. Stefanopoulou, H. Peng, IEEE Transactions on Control Systems Technology 14 (6) (2006).
[13] Y. Zhang, H. Liang, H. Xun, L. Wu, Proceedings of the IEEE Vehicle Power and Propulsion Conference, VPPC 2008, 3–5 September, 2008.
[14] A.F. Burke, Proceedings of the IEEE, vol. 95, Issue. 4, April, 2007.
[15] Z. Cerovsky, P. Mindl, Proceedings of the European Conference on Power Electronics and Applications, EPE 2005, 11–14 September, 2005.
[16] A. Di Napoli, F. Crescimbini, S. Rodo, L. Solero, Proceedings of the IEEE Power Electronics Specialists Conference PESC 2002, Cairns, Australia, June, 2002.
[17] M.B. Camara, H. Gualous, F. Gustin, A. Berthon, IEEE Transactions on Vehicular Technology 57 (September (5)) (2008).
[18] V. Serrao, A. Lidozzi, L. Solero, A. Di Napoli, Proceedings of the European Conference on Power Electronics and Applications, EPE 2007, Aalborg, Denmark, September, 2007.
[19] A. Lidozzi, V. Serrao, L. Solero, F. Crescimbini, Proceedings of the European Conference on Power Electronics and Applications, EPE 2007, Aalborg, Denmark, September, 2007.
[20] A. Lidozzi, L. Solero, F. Crescimbini, A. Di Napoli, IEEE Transactions on Power Electronics 22 (January 1) (2007).
[21] K. Zhou, D. Wang, IEEE Transactions on Industrial Electronics 49 (February (1)) (2002).
[22] L. Solero, A. Lidozzi, J.A. Pomilio, IEEE Transactions on Power Electronics 20 (September–October (5)) (2005).
[23] A. Lidozzi, L. Solero, Proceedings of the IEEE International Symposium on Industrial Electronics, ISIE 2004, Ajaccio, France, May, 2004.